



Research article

Group theoretic particle swarm optimization for gray-level medical image enhancement

Jinyun Jiang^{1,†}, Jianchen Cai^{1,*}, Qile Zhang^{2,†,*}, Kun Lan¹, Xiaoliang Jiang¹ and Jun Wu¹

¹ College of Mechanical Engineering, Quzhou University, Quzhou 324000, China

² Department of Rehabilitation, The Quzhou Affiliated Hospital of Wenzhou Medical University, Quzhou People's Hospital, Quzhou 324000, China

† The authors contributed equally to this work.

* **Correspondence:** Email: cai198666@126.com, zjzhangqile@163.com.

Abstract: As a principal category in the promising field of medical image processing, medical image enhancement has a powerful influence on the intermedia features and final results of the computer aided diagnosis (CAD) system by increasing the capacity to transfer the image information in the optimal form. The enhanced region of interest (ROI) would contribute to the early diagnosis and the survival rate of patients. Meanwhile, the enhancement schema can be treated as the optimization approach of image grayscale values, and metaheuristics are adopted popularly as the mainstream technologies for medical image enhancement. In this study, we propose an innovative metaheuristic algorithm named group theoretic particle swarm optimization (GT-PSO) to tackle the optimization problem of image enhancement. Based on the mathematical foundation of symmetric group theory, GT-PSO comprises particle encoding, solution landscape, neighborhood movement and swarm topology. The corresponding search paradigm takes place simultaneously under the guidance of hierarchical operations and random components, and it could optimize the hybrid fitness function of multiple measurements of medical images and improve the contrast of intensity distribution. The numerical results generated from the comparative experiments show that the proposed GT-PSO has outperformed most other methods on the real-world dataset. The implication also indicates that it would balance both global and local intensity transformations during the enhancement process.

Keywords: medical image enhancement; metaheuristics; group theory; intensity transformation

1. Introduction

As an important substantial part of receiving, processing and analyzing images in the biomedical engineering and science domains, medical image enhancement aims to facilitate the quality of images and prevent them from poor illumination, noise interference and artifact influence, which is essential for detecting various clinical conditions, features, ailments and making suitable diagnostic decisions followed by [1]. As well known, the misdiagnosis of diseases would lead to severe mistakes and further exacerbate the life-threatening situation. Therefore, improving visual perception and machine understanding of medical images is imperative through enhancement technologies in the computer aided diagnosis (CAD) system [2].

Considering the difference between black and white parts in an image, the contrast measures the contradiction of different objective brightest and darkest grayscale values. The display quality depends on the matter of contrast, the higher the contrast, the better the display and vice versa. Under most circumstances, there are noises, distortions and blurs in medical images so that low contrast is observed frequently from those images, which causes the complex and time-consuming action in the next stage of processing. As the enhancement is concerned, it is focused mainly on transferring the input image towards outputting the better one with less noise and more detailed information on intensity distribution [3,4]. To this effect, histogram equalization (HE) technology is one of the early enhancement methods that can adjust the contrast primitively by increasing or decreasing the global intensity of an image [5]. Thus, it always suffers from the problem of over-enhancement when both high and low occurring intensities are combined and transferred together. As a consequence, the bi-histogram equalization (BHE) method is presented to double the histogram and maintain the quality of the original image [6,7]. However, the limitation of BHE cannot be eliminated due to the asymmetrical pixel distribution in the histogram. Furthermore, the adaptive histogram equalization (AHE) contains the non-linear transformation and correction of contrast to overcome the drawbacks of HE and BHE [8], but it becomes less effective when there are complicated differences in the illumination. Besides, enhancement technologies such as contrast limited adaptive histogram equalization (CLAHE), balance contrast enhancement (BCE), gamma correction, texture-cartoon separation and complement techniques are investigated for the effects of enhancing image contrast and brightness [9–12].

According to the subjective nature of the human intervention in image enhancement, the parameter configuration of contrast adjustments is the key to solving enhancement problems at the level of different grayscales [13]. Several metaheuristics are applied in the enhancement domain, Archana et al. [14] presented the improved genetic algorithm (GA) for setting the parameters of contrast transformation with the fitness function of entropy and edge properties. Its results showed better performance than linear contrast stretching (LCS) method. The proposed differential evolution (DE) in Suresh and Lal [15] and Bhandari et al. [16] was appropriately utilized for color images enhancement with the parameters of color quality such as peak signal to noise ratio (PSNR), feature similarity index measure (FSIM), structural similarity index measure (SSIM), etc. And DE outperformed several state-of-the-art methods based on the above measurements. A modified sigmoid function combining the information of edge and entropy cooperates with particle swarm optimization (PSO) [17] to reduce the noise and enhance the quality of grayscale images. The results were better than HE, AHE and GA. A fuzzy framework with S-shape membership function [18] is embedded into PSO to overcome the issues when upgrading the imprecise nature of retinal images. The visual quality

and contrast were increased after the comparative experiments. The weighted vector median filtering-based ant colony optimization (ACO) [19] proved its effort of finding the appropriate transformation where the objective functions are minimum square error (MSE) and minimum absolute error (MAE) [20]. An improved algorithm of monarch butterfly optimization (MBO) [21] was proposed to equalize the distribution of multiple grayscale levels in terms of PSNR and SSIM values, the migration and adjusting operators were refined and a new adaptive crossover rate was adopted to enhance the optimization process. Li et al. [22] presented the slime mould algorithm (SMA) for thresholding-based contrast enhancement, cooperating with the Lévy flight and quasi opposition-based learning method to improve the image quality. Moth swarm algorithm (MSA) [23] optimized the maximum kullback-leibler entropy (KL-entropy) and redistributed the intensities of pixels in the reduced histogram, thus the noisy and irrelevant information would be eliminated and the pixel intensities became more significant in the enhanced image. The dimension learning-based hunting (DLH) search strategy was integrated with harris hawks optimization (HHO) approach [24], which alleviated the lack of premature convergence, crowd diversity and the imbalance between the exploration and exploitation for enhancement optimization. Three core procedures including rule updating, vector combining and a local search were employed for the weighted mean of vectors (WMV) optimizer [25] to filter the noise of the enhanced image, and the results showed better performance than traditional methods. hunger games search (HGS) with dynamic and fitness-wise search methods allowed hunger-driven activities during the contrast optimization process [26], and an adaptive hunger weight was used to simulate the effects of behavioral choices of animals, the results with high quality, fast convergence and stable balance were obtained. Colony predation algorithm (CPA) utilized the mapping functions of animal hunting groups with targeting, dispersing and encircling strategies to search the solution space of image enhancement [27], the success rate was introduced to adjust the cross-border situations for the optimization approach. Rime optimization algorithm (RIME) simulated the soft-rime search mechanism and hard-rime puncture process to generate the optimal solutions [28], the exploitation capability of the population was enhanced by the greedy selection approach for the optimization process. Oloyede et al. [29] conducted the overall comparison of nine metaheuristics involving the most popular algorithms on magnetic resonance imaging (MRI) datasets with the fitness computation rate (FCR) in the fairer sense. They summarized that there was no substantial difference among those methods considering both qualitative and quantitative analyses. However, the pros and cons of the compared methods were not discussed in detail, and the conclusion empirically depended on the particular types of various medical images [30–32].

To sum up briefly, the reviewed literature about the metaheuristics-based medical image enhancement has implicated that the supremacy of different metaheuristics over other existing enhancement technologies is obtained. But more importantly, interactive procedures are required to achieve the satisfactory results and it is unsuitable for routine scenarios. And there are still major challenges of medical image enhancement, for example the selection of various evaluation functions, the satisfaction of different intensity transformations, the employment of multiple grayscale level technologies, etc.

Theoretically, the medical image enhancement task can be formulized as non-linear and multi-modal optimizations in terms of its complicated characteristics. To address these problems, a novel metaheuristic algorithm named group theoretic particle swarm optimization (GT-PSO) [33–35] is presented to provide a new framework of metaheuristics and give a different view of enhancement methods in this research work. With the solid mathematical foundation of symmetric group theory, the

proposed GT-PSO comprising four major components (particle encoding, solution landscape, neighborhood movement and swarm topology) would rebuild the search paradigm for specific optimization tasks. The problem is represented by the particle encoding properly, and the solution landscape is decomposed into four different hierarchical partitions according to symmetric group theory. Under the guidance of corresponding operators of each hierarchical level, GT-PSO can move the particle neighborhoods in a systematical way and upgrade the dynamic particle swarm topology to solve the problem efficiently. The contributions of GT-PSO in this paper are primarily summarized below:

- An innovative framework of metaheuristic search mechanism based on symmetric group theory is proposed for non-linear and multi-modal optimizations
- Both global and local intensity transformations of medical images are considered in the process of enhancement, and the balance between them is maintained during the search
- The hybrid of the transferred image contents of intensity, entropy and edge is designed as the comprehensive fitness function of medical image enhancement

The remainder of this paper is organized below: Section 2 describes the materials and methods of the proposed work; Section 3 displays the experimental results of case studies from MRI datasets; Section 4 analyzes the performance and reasons behind the proposed method; Section 5 concludes the entire paper.

2. Materials and methods

2.1. Methods

2.1.1. Problem formulation

As the main purpose of medical image enhancement, the technology of the intensity-based transformation function is employed to map the brightness values of an input image to a new grayscale matrix in the non-linear form. Therefore, the efficient function is needed for achieving the optimal values of intensity mapping for the enhancement process. The equation of the non-linear transformation function is described as follows.

$$E_{m,n} = T(I_{m,n}) = K_{m,n} \times (I_{m,n} - \gamma \times \mu_{m,n}^l) + (\mu_{m,n}^l)^\alpha \quad (1)$$

where T is the mapping operation of transformation function, $E_{m,n}$ is the enhanced grayscale value at the position of pixel (m,n) of the original image I with the size of (M,N) , α and γ are enhancement related parameters, $K_{m,n}$ is the enhancement factor function and $\mu_{m,n}^l$ is the local mean of pixel (m,n) of the original image over a sliding window with the size of (w,w) .

$$\mu_{m,n}^l = \frac{1}{w \times w} \sum_{m=1}^w \sum_{n=1}^w I_{m,n} \quad (2)$$

$$K_{m,n} = \frac{\delta \times \mu^g}{\sigma_{m,n}^l + \beta} \quad (3)$$

where β and δ are enhancement related parameters, μ^g is the global mean of the original image and $\sigma_{m,n}^l$ is the local standard deviation of pixel (m,n) of the original image.

$$\mu^g = \frac{1}{M \times N} \sum_{m=1}^M \sum_{n=1}^N I_{m,n} \quad (4)$$

$$\sigma_{m,n}^l = \sqrt{\frac{1}{w \times w} \sum_{m=1}^w \sum_{n=1}^w (I_{m,n} - \mu_{m,n}^l)^2} \quad (5)$$

Through the above equations of the transformation function, the contrast of the original image is made to be stretched in the center of its local mean with the range of its local standard deviation. It has brightening and smoothing effects compared to the original one so that the quality of the contrast is improved in terms of both global and local information about the image.

2.1.2. Fitness function

As the cost evaluation of the single objective optimization, the hybrid components of intensity, entropy and edge of a transferred medical image constitute the fitness function during the enhancement process, where the global information of intensity and entropy cooperates with the local content of edge. The fitness function is formulated as the multiplication of the aforementioned three parts as follows.

$$F(E) = \log(\log(S(E))) \times \frac{C(E)}{M \times N} \times H(E) \quad (6)$$

where E is the enhanced image after the transformation in Eq (1), S is the sum of all pixels in E after Sobel edge detection containing the gradient magnitude and direction of the enhanced image.

$$S(E) = \sum_{m=1}^M \sum_{n=1}^N \sqrt{(\Delta_m E_{m,n})^2 + (\Delta_n E_{m,n})^2} \quad (7)$$

where Δ is the Sobel gradient operation.

$$\Delta_m E_{m,n} = (E_{m-1,n+1} + 2E_{m,n+1} + E_{m+1,n+1}) - (E_{m-1,n-1} + 2E_{m,n-1} + E_{m+1,n-1}) \quad (8)$$

$$\Delta_n E_{m,n} = (E_{m-1,n-1} + 2E_{m-1,n} + E_{m-1,n+1}) - (E_{m+1,n-1} + 2E_{m+1,n} + E_{m+1,n+1}) \quad (9)$$

C is the count of non-zero pixels whose intensity value is greater than a certain threshold θ after Sobel edge detection in E .

$$C(E) = \sum_{m=1}^M \sum_{n=1}^N c_{m,n}, \quad c_{m,n} = \begin{cases} 1, & \text{if } \sqrt{(\Delta_m E_{m,n})^2 + (\Delta_n E_{m,n})^2} \geq \theta \\ 0, & \text{if } \sqrt{(\Delta_m E_{m,n})^2 + (\Delta_n E_{m,n})^2} < \theta \end{cases} \quad (10)$$

H is the entropy of E .

$$H(E) = - \sum_{i=0}^{\bar{m}-1} (P_i^E \times \log(P_i^E)) \quad (11)$$

where \bar{m} is maximum value of grayscales in the histogram of E , P_i^E is the observed statistical probability of the occurrence of pixels with i^{th} grayscale quantity in E .

The efficiency of medical image enhancement is facilitated by selecting the optimal parameters

of the fitness function. Basically, it is the optimization problem of combinatorial solutions of multiple parameters that can be mathematically modeled and solved via the proposed GT-PSO. In the following, the GT-PSO methodology will be investigated to tackle this kind of issue in medical image enhancement as the non-linear and multi-modal optimization problems and the target of the corresponding optimization is to maximize the objective function formulated in Eq (1).

2.1.3. Particle encoding

The solution of the optimized problem is encoded in the form of cycles of permutations for each particle of GT-PSO, whose degree equals to the dimension D of the fitness function. The candidates of different solutions are carried out using various permutations of the symmetric group, where p is the mapping operation from one possible value to another for each dimension x_i in the solution.

$$sol = (p(x_1) p(x_2) \dots) \dots (\dots p(x_{D-1}) p(x_D)) \tag{12}$$

2.1.4. Solution landscape

The four layer-based hierarchical decomposition of search landscape is applied to provide the systematic perspective of the whole solution space, which consists of four main components: conjugacy class, cyclic form, orbital plane and orbit, respectively. The hierarchical partitions of the solution space landscape are demonstrated in Figure 1. Note that the hierarchical partitions can ensure the complete and exclusive decomposition of the solution space.

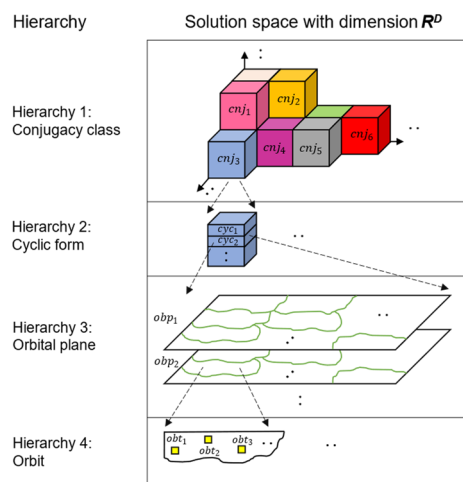


Figure 1. The demonstration of four layer-based hierarchical partitions of the solution landscape.

Conjugacy class is the first-order partition of the hierarchy, and it contains several sequential items with the structure that is similar to the exponential form. i^{k_i} means that there are k_i cycles with the size of i in the conjugacy class.

$$cnj = 1^{k_1} 2^{k_2} \dots i^{k_i} \dots D^{k_D}, \forall i \in [1, D], k_i \in [0, D] \tag{13}$$

$$\sum_{i=1}^D i k_i = D \tag{14}$$

Cyclic form is the second-order partition of the hierarchy, and it has different cyclic factors based on the permutation form. A specific permutation is implemented via the combination of multiple group actions, and each of them is denoted by the notation of the pair of parentheses.

$$cyc = (x_1 x_2 \dots) \dots (\dots x_{D-1} x_D) \tag{15}$$

Orbital plane is the third-order partition of the hierarchy, and it is the collection of all possible elements if the results after two group actions g_1 and g_2 are the same applied to a sequence set X . The sequence set X is the collection of candidates of the solutions.

$$obp = \{X_k\}, \text{ iff } X_i(g_1) = X_i(g_2), \forall i \in [1, k] \tag{16}$$

Orbit is the fourth-order partition of the hierarchy, and it is the aggregation of all possible results after the specific group action g from a given group G . The content of the orbit is determined by different group actions on the sequence set X .

$$obt = \{gx | g \in G\}, \forall x \in X \tag{17}$$

2.1.5. Neighborhood movement

The operations of neighborhood movements of specific particles are manipulated to search the incumbent solutions with the guidance of multiple group action combinations. Based on the hierarchical partitions of four layers, the corresponding four types of operations are carried out. The illustration of details of neighborhood movements with respect to particle update is displayed in Figure 2.

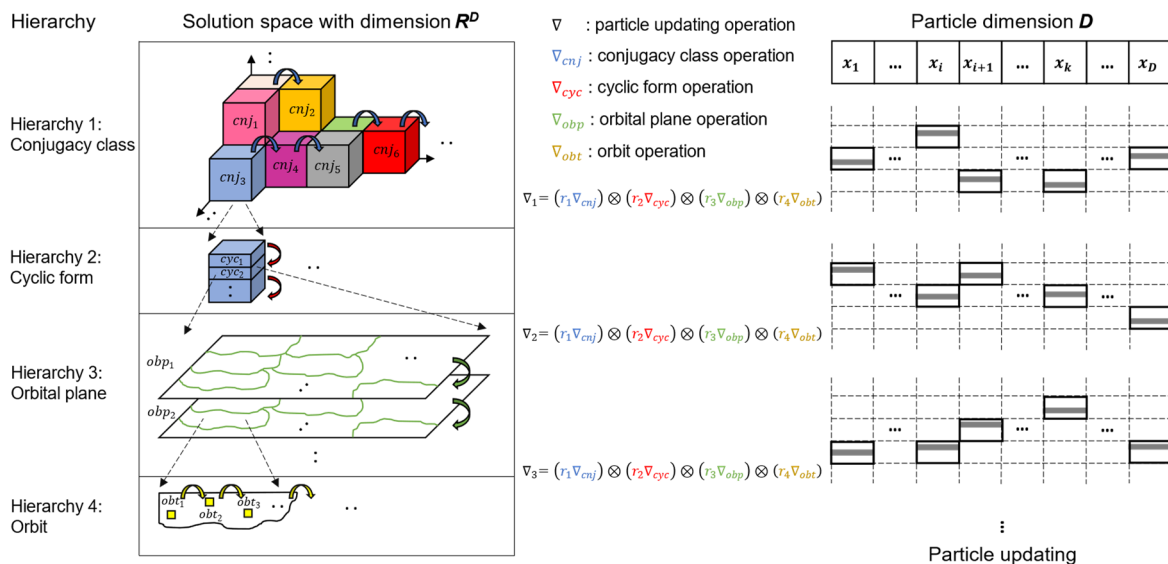


Figure 2. The illustration of neighborhood movement with the guidance trends of hierarchical operations of four layers.

The yellow arrows are the orbiter operations that can search along the orbits consecutively within one orbital plane, and the green arrows are the orbital planer operations that would change the orbital plane from one to another within one cyclic form. Meanwhile, the red arrows are the cycler operations that could move across different cyclic forms within the one conjugacy class, and the blue arrows are

the conjugator operations that may jump over various conjugacy classes in the solution space. The previous two operations of orbiter and orbital planer belong to the category of search exploitation during the optimization to facilitate the ability of intensification, and the latter two operations of cycler and conjugator belong to the category of search exploration during the optimization to enhance the capacity of diversification.

2.1.6. Swarm topology

The swarm topology for updating all particles after neighborhood movements is formulated below. Let ∇ denote the operation generated by group action combinations via group multiplication \otimes , the evolutionary formulae of the whole swarm are induced.

$$\nabla = (r_1 \nabla_{cnj}) \otimes (r_2 \nabla_{cyc}) \otimes (r_3 \nabla_{obp}) \otimes (r_4 \nabla_{obt}) \quad (18)$$

$$v_{k+1}^i = \nabla \otimes v_k^i + r_5 \times c_1 \times (p_k^i - x_k^i) + r_6 \times c_2 \times (p_k^g - x_k^i) \quad (19)$$

$$x_{k+1}^i = x_k^i + v_{k+1}^i \quad (20)$$

where r_1 to r_6 are the random numbers, c_1 and c_2 are the acceleration coefficients, k is the iteration number, i is the particle index, p_k^i is the local best fitness value of the objective function of i^{th} particle after k iterations while p_k^g is the global best one.

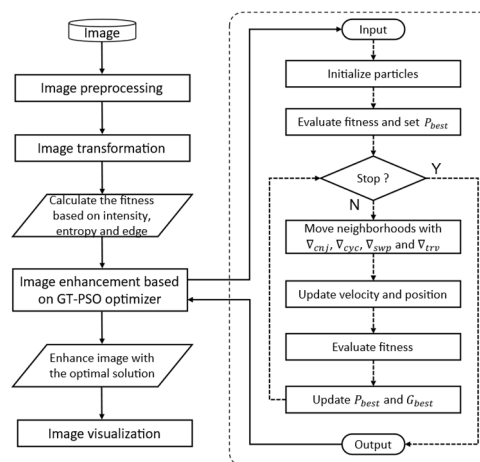


Figure 3. The flowchart of image enhancement with GT-PSO optimizer.

Equation (18) shows the concurrent cooperation of four operations from different hierarchical layers and the velocity upgrade of a single particle. The new velocity and final position of a particle are obtained in Eqs (19) and (20), respectively. The overall workflow of the proposed GT-PSO as the image enhancement optimizer is observed in Figure 3 simultaneously. The input images will be preprocessed and transferred to the proper format, whereby the GT-PSO optimizer calculates the fitness score of the hybrid of the transferred contents and searches for the optimal solutions. The search stops when certain conditions are satisfied, for instance the minimal error rate is reached, or the maximal number of iterations is counted.

2.2. Materials

The materials used in this paper are chosen from the MedPix dataset presented by the National Library of Medicine, which is a free and open access online database covering many types of clinical materials. Within this database, the medical images are categorized into different groups such as cardiovascular, pulmonary, abdomen, chest, eye orbit, brain neuro, etc. The selected case comprises a contrast enhanced axial computed tomographic (CT) scan of the disease of acute appendicitis, and the case study containing 1000 images is conducted to test the effects of gray-level enhancement by the proposed GT-PSO compared to other alternative metaheuristic methods like GA, ACO, PSO and DE. The configuration of parameters of those comparative algorithms is listed in Table 1 with the empirical studies from a wide range of research works. In order to make the comparisons between the proposed and alternative methods more meaningful, the pairwise non-parametric Wilcoxon's rank sum test is carried out to determine the statistical significance of those comparisons. The significance level α is 0.05 and the number of independent runs of each comparative method is 30.

Table 1. The parameter setting of the comparative methods.

Method	Parameter	Value
Fitness	Input image size	512
	Sliding window size	5
GA	Population size	30
	Crossover rate	0.5
	Mutation rate	0.15
ACO	Population size	30
	Pheromone factor	1.0
	Heuristic factor	1.5
	Evaporation rate	0.3
PSO	Population size	30
	Inertial weight	1.0
	Acceleration coefficient	2.0
DE	Population size	30
	Crossover rate	0.5
	Low bound	0.3
	High bound	0.6
INFO	Population size	30
	Exponential coefficient	2
	Generation distance	4
HHO	Population size	30
	Control parameter	2.5
	Scaling factor	0.5
GT-PSO	Population size	30
	Random 1&2	0.5
	Random 3&4	0.6
	Random 5&6	0.4
	Acceleration coefficient	2.0

3. Results

In the case study of the real-life application of acute appendicitis in MedPix, the example of an original image coded “synpic28644” is illustrated in Figure 4(a),(b) shows the enhanced example of the same image by the proposed GT-PSO. In Figure 4(a), there exists the distended appendix with thickened enhancing walls in ROI, as well as the changes of periappendiceal inflammatory with fat stranding. In Figure 4(b), it depicts that the better boundaries of the lesion in the target organ are delineated than in Figure 4(a). The brightness around the boundaries of the wall protruding to the caecum gets enhanced so that the contrast is more vivid and the radiologist could provide an advanced diagnostic procedure.

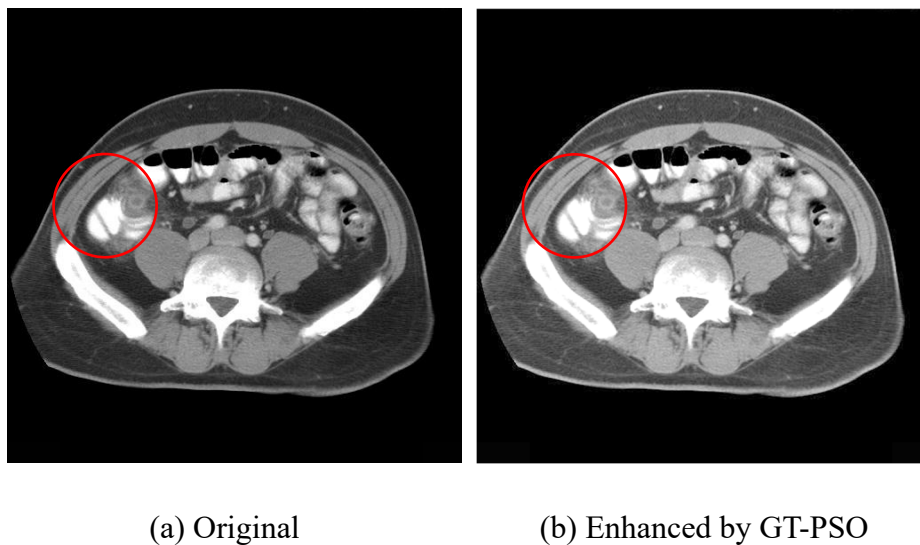


Figure 4. The illustration of acute appendicitis with the original example and the enhanced one by GT-PSO from MedPix.

The fitness score obtained from the fitness function is the main factor in measuring the performance of those comparative methods, followed by another performance metric of the convergence rate shown in Figure 5. In detail, the numerical results of fitness scores involve mean, standard deviation, best values from 30 independent runs of 2000 tested CT images and p-values between two comparative methods of the hypothesis test are tabulated in Table 2. It can be observed that the proposed GT-PSO outperforms the rest of the alternative algorithms and the results from Figure 5 and Table 2 can prove the conclusion mutually. In all situations, GT-PSO has the superior averaged fitness score of 11.885 that is 4.2% higher than the worst case of GA, its performance is also evidenced by the best values in Table 2. HHO has the second best averaged fitness score, followed by DE, INFO and PSO and ACO performs almost equivalently to GA. The standard deviation of GT-PSO is 0.358 which is nearly the lowest value of all except DE and the result indicates that the distribution of the fitness scores of GT-PSO is very converged while ACO gets the scattered distribution. As far as the p-value is concerned, there is indeed significant difference between pairwise comparison of two algorithms if the result is less than the threshold of the significance level. All the p-values of GT-PSO and other methods are less than 0.05, thus GT-PSO is statistically better than others in terms of the balance between random nature and systematic behaviour by symmetric group theory.

Table 2. The measure of mean, standard deviation, best and p-value of fitness scores of the comparative methods.

Measure	GA	ACO	PSO	DE	HHO	INFO	GT-PSO
Mean	11.407	11.449	11.732	11.810	11.854	11.798	11.885
Std	0.547	0.556	0.437	0.341	0.483	0.416	0.358
Best	11.829	11.887	11.932	12.165	12.354	12.214	12.286
P-value	0.000	0.000	0.000	0.005	0.023	0.016	/

The visualization of fitness scores of comparative methods over iteration numbers is displayed in Figure 5. The results represented by those curves in different describe the convergence trends of each method. The total number of iterations is set to be 1000 and after 800 iterations all methods get converged in the latter phase of the search process. Compared to other methods, GT-PSO shows the rapid convergence speed and high convergence rate in the initial phase and converges finally around 500 iterations, which is much earlier than others. ACO performs the lower fitness score but the faster convergence rate in the initial phase and GA converges stably during the most majority of the search process. DE has a good convergence speed and convergence rate and would achieve the optimum performance before 800 iterations, while the PSO curve shares a similar shape compared to GT-PSO but its result is medium among all. The convergence speed of HHO is faster than GT-PSO in the initialization stage around 50 iterations, but it performs worse than GT-PSO finally. INFO is superior to DE but worse than GT-PSO and HHO.

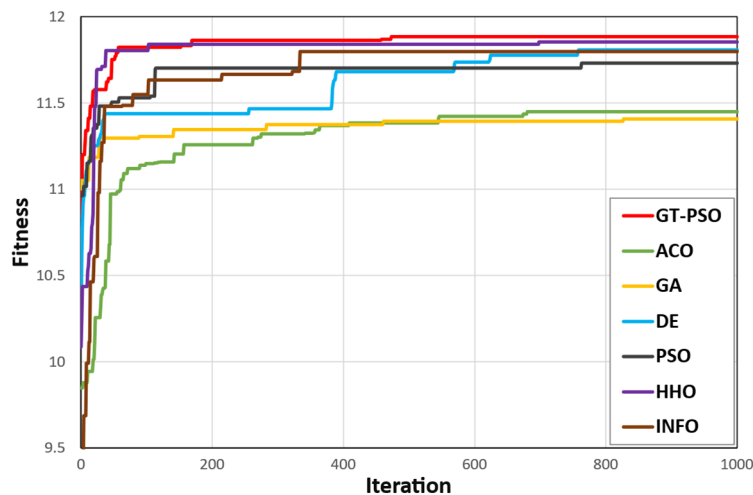


Figure 5. The visualization of fitness score curves of comparative methods over iterations.

4. Discussion

Generally speaking, the image enhancement is the optimization problem with NP-hard feature and the experimental results reveal that all comparative metaheuristics could tackle this type of problem using their own search strategies. More specifically, the population-based metaheuristics utilize the trial-and-error mechanism of the collaborative search of multiple agents and the approximation approach of random access. Besides that, it is worth mentioning that the proposed GT-

PSO comprises an extra mathematical framework of symmetric group theory, therefore that is the reason why GT-PSO outperforms others on medical image datasets. Theoretically, the search paradigm of GT-PSO is classified into the categories of intensification and diversification via the operations of hierarchical partitions and the adaptive parameter configuration of the swarm topology. In Figure 5, GT-PSO gets converged towards the global optimum rapidly due to the concentration on intensification implemented by orbital planer and orbiter operations in the previous iterations around 100, meanwhile it works stably in the latter iterations around 500 because of the focus of diversification achieved by conjugator and cycler operations. The stagnation at the local optimum is prevented through the balanced control of parameters when the dimension of the objective function increases severely. However in this case study, the dimension of the optimization problem is not so large, so the GT-PSO would converge soon. Then the implication of GT-PSO convergence performance is interpreted according to the theory of symmetric group.

For the discussion of the rest of the comparative methods, GA curve (in yellow) suffers from the limitation of the consequence of early maturing that is stuck in the local stagnation around 50 iterations with the less optimum result. The reason behind this case may reside in the complex operations of selection, crossover, mutation and the determination of a large number of parameters during the search correspondingly. ACO curve (in green) has inferior performance than other methods because the positive feedback of accumulated pheromones of the solution candidates would descend the escape strategies of multiple agents to generate the potential solutions with better quality, and furthermore the bad ones occupy the majority of all solutions. The shape of PSO curve (in black) is like the GT-PSO since it is the extension of PSO with the refined foundation of symmetric group theory, basically they share some features of the search paradigm in common. DE curve (in blue) could improve the convergence obviously in the middle stage of the search because there are solid foundations of adaptive dynamic turbulence strategies during the differential evolution approaches that may lead to a fairly decent performance compared to other algorithms. HHO curve (in purple) could cooperatively pounce the optimal target from different directions and escape from various dangers, so a variety of chasing patterns containing diversification and intensification are mimicked to generate the superior performance. INFO curve (in brown) uses updating rule and vector combining steps to increase the capacities of exploitation and exploration, but the local search limits its converging performance in the initialization stage.

The time complexity of the proposed GT-PSO is analyzed as follows. Suppose that D is the parameter dimension of the fitness function in Eq (1), Cof is the evaluation cost of the fitness function in Eq (1), P is the size of swarm population and K is the number of iterations. The time complexity of Cof is $O(D)$ since those independent parameters are the linear sequences that constitute the fitness function in Eq (1). The time complexity of the initialization stage of GT-PSO is $T_{ini} = O(P * D + P * Cof) = O(P * D)$, and the time complexity of GT-PSO operations in iteration stage is $T_{opt} = T_{cnj} + T_{cyc} + T_{obp} + T_{obt} = O(P * D)$. So the total time complexity is $O[K * P * (D + Cof)] = O(K * P * D)$, which is polynomial and acceptable for NP-hard problem solutions.

The space complexity of the proposed GT-PSO is discussed as follows. Similar to time complexity, the space complexity of the initialization stage of GT-PSO is $S_{ini} = O(P * D + P * Cof) = O(P * D)$, the space complexity of the search stage of GT-PSO is $S_{opt} = S_{cnj} + S_{cyc} + S_{obp} + S_{obt} = O(P * D)$, thus the total space complexity is $O[P * (D + Cof)] = O(P * D)$ and the iteration number K is excluded compared to the analysis of the time complexity.

5. Conclusions

The gray-level image enhancement problem remains a continuous challenge and a longstanding issue to be addressed in the field of medical image analysis research. We propose the novel metaheuristic algorithm named Group Theoretic Particle Swarm Optimization (GT-PSO) based on the solid mathematical foundation of symmetric group theory to provide a new search paradigm. It consists of four systematic parts including particle encoding, solution landscape, neighborhood movement and swarm topology. The enhancement problem is formulated and the combined objective function on the grayscale level of pixels is designed correspondingly. Our proposed method is tested by using a real-world dataset and compared with other classic and practical optimization algorithms in the experiments. The results show that GT-PSO outperforms all other selected conventional metaheuristics methods, which proves that GT-PSO has the potential for further research of real-life applications with good quality and great value of related theoretical studies. Although GT-PSO has achieved many advantages, there are still some limitations of the existing algorithm. It can not guarantee to reach the global optimum theoretically because of the essentials of metaheuristics, and the enormous computational time is caused when objective functions become highly complex.

The future works may include but not limited to the following tasks. A further investigation of the mapping function to transfer discrete and continuous representations so that more continuous optimization problems can be solved by GT-PSO. The balanced relationship between diversification and intensification could be enhanced by the incremental strategy of parameter configuration. As a step forward, the theories of Lie group and fiber bundles can be applied to enrich the mathematical foundations of metaheuristics frameworks. The improved GT-PSO would be utilized to address the multi-objective optimization problems.

Acknowledgments

This work was supported by the National Natural Science Foundation of China (Nos. 62102227, 51805124, 62101206), Zhejiang Basic Public Welfare Research Project (Nos. LZYZ22E050001, LZYZ22D010001, LGG19E050013, LZYZ21E060001, TGS23E030001, LTGC23E050001), Science and Technology Major Projects of Quzhou (2021K29, 2022K56).

Conflict of interest

The authors declare there is no conflict of interest.

References

1. S. Chakraborty, K. Mali, S. Chatterjee, S. Banerjee, A. Sah, S. Pathak, et al., Bio-medical image enhancement using hybrid metaheuristic coupled soft computing tools, in *2017 IEEE 8th Annual Ubiquitous Computing, Electronics and Mobile Communication Conference (UEMCON)*, (2017), 231–236. <https://doi.org/10.1109/UEMCON.2017.8249036>
2. N. Du, Q. Luo, Y. Du, Y. Zhou, Color image enhancement: A metaheuristic Chimp optimization algorithm, *Neural Process. Lett.*, **54** (2022), 4769–4808. <https://doi.org/10.1007/s11063-022-10832-7>

3. W. Wang, C. Zhang, Bifurcation of a feed forward neural network with delay and application in image contrast enhancement, *Math. Biosci. Eng.*, **17** (2020), 387–403. <https://doi.org/10.3934/mbe.2020021>
4. S. Chakraborty, A. Raman, S. Sen, K. Mali, S. Chatterjee, H. Hachimi, Contrast optimization using elitist metaheuristic optimization and gradient approximation for biomedical image enhancement, in *2019 Amity International Conference on Artificial Intelligence (AICAI)*, (2019), 712–717. <https://doi.org/10.1109/AICAI.2019.8701367>
5. M. J. Horry, S. Chakraborty, B. Pradhan, M. Fallahpoor, H. Chegeni, M. Paul, Factors determining generalization in deep learning models for scoring COVID-CT images, *Math. Biosci. Eng.*, **18** (2021), 9264–9293. <https://doi.org/10.3934/mbe.2021456>
6. R. Janarthanan, E. A. Refaee, K. Selvakumar, M. A. Hossain, R. Soundrapandiyar, M. Karuppiah, Biomedical image retrieval using adaptive neuro-fuzzy optimized classifier system, *Math. Biosci. Eng.*, **19** (2022), 8132–8151. <https://doi.org/10.3934/mbe.2022380>
7. J. R. Tang, N. A. M. Isa, Bi-histogram equalization using modified histogram bins, *Appl. Soft Comput.*, **55** (2017), 31–43. <https://doi.org/10.1016/j.asoc.2017.01.053>
8. U. K. Acharya, S. Kumar, Genetic algorithm based adaptive histogram equalization (GAAHE) technique for medical image enhancement, *Optik*, **230** (2021), 166273. <https://doi.org/10.1016/j.ijleo.2021.166273>
9. T. Rahman, A. Khandakar, Y. Qiblawey, A. Tahir, S. Kiranyaz, S. B. A. Kashem, et al., Exploring the effect of image enhancement techniques on COVID-19 detection using chest X-ray images, *Comput. Biol. Med.*, **132** (2021), 104319. <https://doi.org/10.1016/j.compbiomed.2021.104319>
10. A. Qayyum, W. Sultani, F. Shamshad, R. Tufail, J. Qadir, Single-shot retinal image enhancement using untrained and pretrained neural networks priors integrated with analytical image priors, *Comput. Biol. Med.*, **148** (2022), 105879. <https://doi.org/10.1016/j.compbiomed.2022.105879>
11. R. Kumar, A. K. Bhandari, Spatial mutual information based detail preserving magnetic resonance image enhancement, *Comput. Biol. Med.*, **146** (2022), 105644. <https://doi.org/10.1016/j.compbiomed.2022.105644>
12. M. Jalali, H. Behnam, M. Shojaeifard, Echocardiography image enhancement using texture-cartoon separation, *Comput. Biol. Med.*, **134** (2021), 104535. <https://doi.org/10.1016/j.compbiomed.2021.104535>
13. K. G. Dhal, S. Ray, A. Das, S. Das, A survey on nature-inspired optimization algorithms and their application in image enhancement domain, *Arch. Comput. Methods Eng.*, **26** (2019), 1607–1638. <https://doi.org/10.1007/s11831-018-9289-9>
14. S. Goel, A. Verma, N. Kumar, Gray level enhancement to emphasize less dynamic region within image using genetic algorithm, in *2013 3rd IEEE International Advance Computing Conference (IACC)*, (2013), 1171–1176. <https://doi.org/10.1109/IAdCC.2013.6514393>
15. S. Suresh, S. Lal, Modified differential evolution algorithm for contrast and brightness enhancement of satellite images, *Appl. Soft Comput.*, **61** (2017), 622–641. <https://doi.org/10.1016/j.asoc.2017.08.019>
16. A. K. Bhandari, A. Kumar, S. Chaudhary, G. K. Singh, A new beta differential evolution algorithm for edge preserved colored satellite image enhancement, *Multidimension. Syst. Signal Process.*, **28** (2017), 495–527. <https://doi.org/10.1007/s11045-015-0353-4>

17. H. K. Verma, S. Pal, Modified sigmoid function based gray scale image contrast enhancement using particle swarm optimization, *J. Inst. Eng. India Ser. B*, **97** (2016), 243–251. <https://doi.org/10.1007/s40031-014-0175-z>
18. S. K. Ghosh, B. Biswas, A. Ghosh, A novel approach of retinal image enhancement using PSO system and measure of fuzziness, *Procedia Comput. Sci.*, **167** (2020), 1300–1311. <https://doi.org/10.1016/j.procs.2020.03.446>
19. H. Gao, W. Zeng, Color image enhancement based on Ant Colony Optimization Algorithm, *Telkomnika*, **13** (2015), 155–163. <http://doi.org/10.12928/telkomnika.v13i1.1274>
20. H. Singh, A. Kumar, L. K. Balyan, A sine-cosine optimizer-based gamma corrected adaptive fractional differential masking for satellite image enhancement, in *Harmony Search and Nature Inspired Optimization Algorithms*, Springer, (2019), 633–645. https://doi.org/10.1007/978-981-13-0761-4_61
21. Y. Feng, S. Deb, G. G. Wang, A. H. Alavi, Monarch butterfly optimization: a comprehensive review, *Expert Syst. Appl.*, **168** (2021), 114418. <https://doi.org/10.1016/j.eswa.2020.114418>
22. S. Li, H. Chen, M. Wang, A. A. Heidari, S. Mirjalili, Slime mould algorithm: A new method for stochastic optimization, *Future Gener. Comput. Syst.*, **111** (2020), 300–323. <https://doi.org/10.1016/j.future.2020.03.055>
23. Y. Feng, G. G. Wang, A binary moth search algorithm based on self-learning for multidimensional knapsack problems, *Future Gener. Comput. Syst.*, **126** (2022), 48–64. <https://doi.org/10.1016/j.future.2021.07.033>
24. A. A. Heidari, S. Mirjalili, H. Faris, I. Aljarah, M. Mafarja, H. Chen, Harris hawks optimization: Algorithm and applications, *Future Gener. Comput. Syst.*, **97** (2019), 849–872. <https://doi.org/10.1016/j.future.2019.02.028>
25. I. Ahmadianfar, A. A. Heidari, S. Noshadian, H. Chen, A. H. Gandomi, INFO: An efficient optimization algorithm based on weighted mean of vectors, *Expert Syst. Appl.*, **195** (2022), 116516. <https://doi.org/10.1016/j.eswa.2022.116516>
26. Y. Yang, H. Chen, A. A. Heidari, A. H. Gandomi, Hunger games search: Visions, conception, implementation, deep analysis, perspectives, and towards performance shifts, *Expert Syst. Appl.*, **177** (2021), 114864. <https://doi.org/10.1016/j.eswa.2021.114864>
27. J. Tu, H. Chen, M. Wang, A. H. Gandomi, The colony predation algorithm, *J. Bionic Eng.*, **18** (2021), 674–710. <https://doi.org/10.1007/s42235-021-0050-y>
28. H. Su, D. Zhao, A. A. Heidari, L. Liu, X. Zhang, M. Mafarja, et al., RIME: A physics-based optimization, *Neurocomputing*, **532** (2023), 183–214. <https://doi.org/10.1016/j.neucom.2023.02.010>
29. M. O. Oloyede, A. J. Onumanyi, H. Bello-Salau, K. Djouani, A. Kurien, Exploratory analysis of different metaheuristic optimization methods for medical image enhancement, *IEEE Access*, **10** (2022), 28014–28036. <https://doi.org/10.1109/ACCESS.2022.3158324>
30. J. Tang, J. Kim, E. Peli, Image enhancement in the JPEG domain for people with vision impairment, *IEEE. Trans. Biomed. Eng.*, **51** (2004), 2013–2023. <https://doi.org/10.1109/TBME.2004.834264>
31. J. Tang, X. Liu, Q. Sun, A direct image contrast enhancement algorithm in the wavelet domain for screening mammograms, *IEEE. J. Sel. Top. Signal Process.*, **3** (2009), 74–80. <https://doi.org/10.1109/JSTSP.2008.2011108>

32. X. Liu, J. Tang, X. Zhang, A multiscale image enhancement method for calcification detection in screening mammograms, in *2009 16th IEEE International Conference on Image Processing (ICIP)*, (2009), 677–680. <https://doi.org/10.1109/ICIP.2009.5414077>
33. K. Lan, G. Li, Y. Jie, R. Tang, L. Liu, S. Fong, Convolutional neural network with group theory and random selection particle swarm optimizer for enhancing cancer image classification, *Math. Biosci. Eng.*, **18** (2021), 5573–5591. <https://doi.org/10.3934/mbe.2021281>
34. S. Fong, K. Lan, P. Sun, S. Mohammed, J. Fiaidhi, A time-series pre-processing methodology for biosignal classification using statistical feature extraction, in *Proceedings of the 10th IASTED International Conference on Biomedical Engineering (Biomed'13)*, (2013), 207–214. <https://doi.org/10.2316/P.2013.791-100>
35. K. Lan, J. Zhou, X. Jiang, J. Wang, S. Huang, J. Yang, et al., Group theoretic particle swarm optimization for multi-level threshold lung cancer image segmentation, *Quant. Imaging. Med. Surg.*, **13** (2023), 1312–1322. <https://doi.org/10.21037/qims-22-295>



AIMS Press

©2023 the Author(s), licensee AIMS Press. This is an open access article distributed under the terms of the Creative Commons Attribution License (<http://creativecommons.org/licenses/by/4.0>)